CHAPTER 4: FATIGUE

Pietro Croce[1], Maria Luisa Beconcini[1], Carlos Lara[2], Daniele Pellegrini[1], Peter Tanner[2]

[1]Department of Civil and Industrial Engineering – Structural Division – Univ. of Pisa, Italy
[2]Eduardo Torroja Institute for Construction Sciences, IETcc-CSIC, Madrid, Spain

Summary

Fatigue is one the most relevant cause of failure of infrastructures or part of them, like bridges, cranes and machinery, offshore structures and so on. A lot of existing structures, mainly built before the 1980, have been designed using inappropriate fatigue classification of details or underestimating the aggressiveness of actual load spectra, so that they are subject to high fatigue failure risk, as demonstrated by fatigue cracks detected even recently in several structures. Fatigue assessment and evaluation of residual fatigue life is then a key topic in verification of existing infrastructure, also in view of designing repair interventions of fatigue damaged details and planning of future maintenance and inspection programmes.

1 INTRODUCTION

Fatigue is one the most relevant cause of failure of infrastructures or part of them, like bridges, cranes and machinery, offshore structures and so on.

As known, *fatigue is the progressive, localised and permanent structural change occurring in a material subjected to conditions that produce fluctuating stresses and strains at some point or points and that may culminate in cracks or complete fracture after a sufficient number of fluctuations* [1] [2].

In engineering structures, fatigue is induced by actions and loads varying with time and/or space and/or by random vibrations. Thus fatigue can be originated by natural events, like waves, wind and so on, or by loads deriving from the normal use of the structure itself, as it happens in bridges, under the action of lorries or trains crossing the bridges themselves.

Unfortunately, millions of existing structures, mainly built before the 1980, have been designed using inappropriate fatigue classification of details or underestimating the aggressiveness of actual load spectra, so that they are subject to high fatigue failure risk, as demonstrated by fatigue cracks detected even recently in several structures.

On the other hand, in the last 30 years, the fatigue behaviour of typical details has been studied so extensively that quite sound knowledge is now available in designing new structures.

Fatigue assessment and evaluation of residual fatigue life is then a key topic in verification of existing infrastructure, also in view of designing repair interventions of fatigue damaged details and planning of future maintenance and inspection programmes. An exhaustive discussion of this relevant subject is outside the scope of the present paper, therefore in the following only some significant aspect is sketched.

First of all, it must be highlighted that the evaluation of the actual fatigue damage requires the knowledge that is the a posteriori reconstruction of the load cycles which acted on the structure during its past life. As for new structures, fatigue loads can be given in terms of

load spectrum, expressing the load variation or the number of recurrences of each load level during the design life of the structure; load spectrum can be expressed by means an appropriate function, graph, histogram or table, deduced from recorded data or by comparison with similar structures. Whenever, as it happens for bridge, the actual load spectrum results so complicated that cannot be directly employed for fatigue checks, it can be replaced by some conventional load spectrum, aimed to reproduce the fatigue induced by the real one.

The evaluation of conventional load spectra is particularly thorny, because it requires considering the actions from the resistance point of view also. In fact, fatigue depends on the nature of the varying actions and loads, and additionally on structural material details, through the shape and the properties of the relevant mechanical fatigue models. When constant amplitude endurance (fatigue) limit $\Delta\sigma_D$ does not exist, like concrete, steel reinforcement or pre-stressing steel in r.c. details, conventional equivalent load spectra, reproducing the actual fatigue damage, are generally adopted, on the contrary, for structural steel or aluminium details, characterized by constant amplitude fatigue limit, it needs to distinguish between equivalent load spectra, reproducing the actual fatigue damage, and frequent load spectra, reproducing the maximum load range significant for fatigue, accordingly as fatigue verifications require cumulative damage computations or boundless fatigue life assessments [3].

In some kind of structures, like offshore structures or cranes and machinery, fatigue load spectra can be often obtained applying the powerful methods of the stochastic process theory, so that the link between the actions and the effects can be expressed by simple formulae, but these methods cannot be applied to bridges, as road or railway traffic loads induce broad band stress histories.

2 FATIGUE MODELS

In the classical approach two kind of fatigue phenomena are generally distinguished, depending on the level of stresses and on the extension of plastic area.

When the notional stress, that is disregarding the stress concentrations, are in the elastic field and the extension of the plasticized zone is very small if compared with the typical dimensions of the detail, being limited, for instance, in the vicinity of stress concentrators or at the apex of the cracks, the number of cycles to failure is high and the phenomenon is identified as *true fatigue* or *high-cycle fatigue*; on the contrary, when dimensions of plasticized zone are comparable with the typical dimensions of the detail, the number of cycles to failure is low and the phenomenon is identified as *low-cycle fatigue*.

Two types of fatigue models (summarized in the following) are generally used for the description of fatigue failures caused by fluctuating actions:

– *S-N* model based on experiments
– Fracture mechanics model

2.1 S-N Approach

An *S-N* curve or Wöhler curve is a relation between the stress range under constant amplitude loading and the number of stress cycles to failure.

Generally, the fatigue curves are reported in the $\log(\Delta\sigma)$-$\log N$ plane, commonly called *S-N* plane.

The complete Wöhler curve (Figure 1) intersects the *S*-axis for N=0,5 (a semi-cycle) at $\Delta\sigma_R$, corresponding to the static resistance of the material. The part of the curve identified by

$N<10^4$ corresponds to the *low-cycle fatigue* interval; the part of the curve identified by $10^5<N<10^6 \div 10^7$ corresponds to the *high-cycle fatigue* interval; the part of the curve identified by $N>10^6 \div 10^7$ corresponds to the constant amplitude limit, if any; while the interval $10^4<N<10^5$ is the transition zone. The extension of rounded knee of the curve corresponding to $N=10^6 \div 10^7$ is usually very small, and can be disregarded.

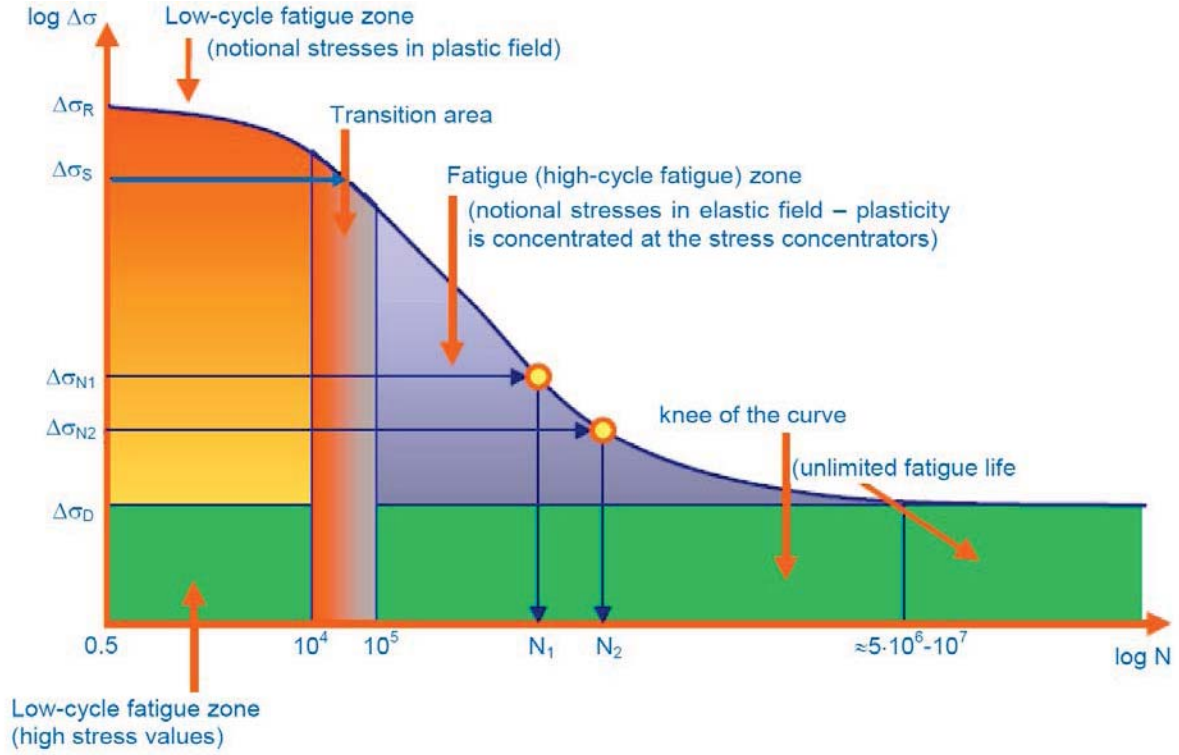

Figure 1 Complete Wöhler curve

In the *high-cycle fatigue* interval, the standard *S-N* curve is linear and it can be expressed in the form:

$$N\,\Delta\sigma^m = A \tag{1}$$

where N is the number of stress cycles to failure at a constant amplitude stress range $\Delta\sigma$, A and m are the material parameters.

In the logarithmic *S-N* chart Wöhler curve pertaining to steel details, characterised by endurance limit, are represented by a bilinear curve, characterised by a sloping branch of constant slope, m=3 (Figure 2) plus a horizontal branch, which is adopted for constant amplitude stress histories or for boundless fatigue life assessments; but, when fatigue damage is to be assessed for stress spectra characterized by varying amplitude of stress cycles, trilinear curves are introduced, characterised by two sloping branches, m_1=3 and m_2=5, (Figure 3) to take into account the influence of pre-existing fatigue damage [4] [5]. In this latter case, a cut-off limit $\Delta\sigma_L$ is introduced, corresponding at 10^8 stress cycles, which is the minimum stress range able to produce fatigue damage in a damaged detail.

In the *low-cycle fatigue* interval, instead in terms of constant stress amplitude, the material behaviour is better expressed in terms of constant plastic strain $\Delta\varepsilon_{apl}$, using the expression experimentally derived by Manson [4] and Coffin [5], whose mathematical formulation is similar to (1)

$$N^k\,\Delta\varepsilon_{apl} = C \tag{2}$$

where N is the number of cycle to failure and k and C are material constants. Equation (2) is usually called Manson-Coffin law.

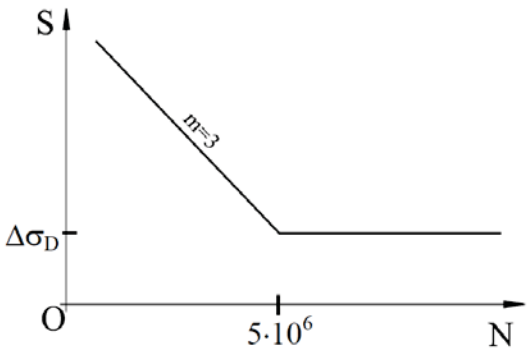

Figure 2 Bi-linear *S-N* curve

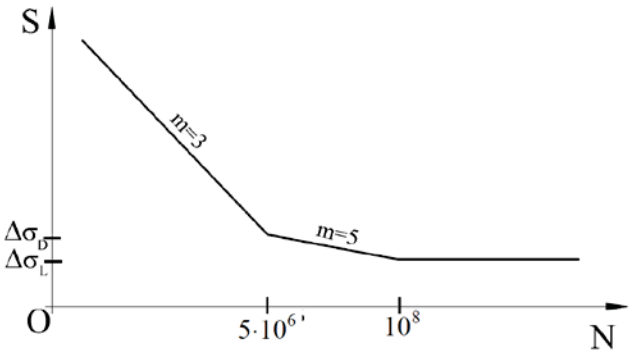

Figure 3 Tri-linear *S-N* curve

Usually, steel details are classified in fatigue using the detail category, which is the characteristic value of the fatigue resistance at $2\cdot10^6$ cycles, allowing to fully define the corresponding bi-linear or tri-linear curve. In Table 1, an example of classification of orthotropic steel deck details is reported, as derived from EN1993-1-9 [6] and EN1993-2 [7].

Unless differently stated, the *S-N* curve of a given structural detail is usually plotted in terms of notional stresses that is disregarding peak stresses, whose theoretical and experimental measure requires ad hoc additional rules. The effects of weld geometry, residual stresses and through thickness stress variation are usually implicitly included in the *S-N* curve, while the effect of other factors such as, plate thickness, environment, weld toe grinding and post-weld heat or mechanical treatments, etc. is accounted through appropriate corrections to the basic *S-N* curve.

In Eurocode EN1999-1-3 [8], bi-linear and tri-linear *S-N* curves are similarly assigned for aluminium structures, but parameters A_1 and m_1, A_2 and m_2, are different: in fact, the slope m_1 can assume the values m_1=3.4 or m_1=4.3, according to the detail under examination, while, as usual, $m_2=m_1+2$.

Other bi-linear models with two sloping lines, characterized by varying parameters A_1 and m_1, A_2 and m_2, $m_2=m_1+2$, are also commonly used for steel reinforcements or for pre-stressing steel details, which does not exhibit fatigue limit [9], [10].

In order to deal with variable amplitude loading, fatigue damage is quantified in terms of Palmgren-Miner's damage summation [11], [12]. Thus, all stress cycles cause a proportional fatigue damage, which is linearly additive.

The total damage D due to a stress spectra composed by k blocks of n_i cycles at stress range $\Delta\sigma_i$, i=1, 2, .., k, is given by:

$$D=\sum_{i=1}^{k}\frac{n_i}{N_i} \tag{3}$$

where N_i is the number of cycles to failure at stress amplitude $\Delta\sigma_i$.

In Equation (3) the material constants can be made explicit, so that it becomes

$$D=\frac{1}{A_1}\sum_{\Delta\sigma_i\geq\Delta\sigma_D} n_i\,\Delta\sigma_i^{m_1}+\frac{1}{A_2}\sum_{\Delta\sigma_D>\Delta\sigma_i>\Delta\sigma_L} n_i\,\Delta\sigma_i^{m_2} \tag{4}$$

Table 1 Fatigue classification of orthotropic steel deck bridge details (EN1993-2)

Detail category	Constructional detail	Description	Requirements
80 71	t≤12mm t>12mm	1) Continuous longitudinal stringer, with additional cutout in cross girder.	1) Assessment based on the direct stress range Δσ in the longitudinal stringer.
80 71	t≤12mm t>12mm	2) Continuous longitudinal stringer, no additional cutout in cross girder.	2) Assessment based on the direct stress range Δσ in the stringer.
36		3) Separate longitudinal stringer each side of the cross girder.	3) Assessment based on the direct stress range Δσ in the stringer.
71		4) Joint in rib, full penetration butt weld with steel backing plate.	4) Assessment based on the direct stress range Δσ in the stringer.
112 90 80	As detail 1, 2, 4 in Table 8.3 As detail 5, 7 in Table 8.3 As detail 9, 11 in Table 8.3	5) Full penetration butt weld in rib, welded from both sides, without backing plate.	5) Assessment based on the direct stress range Δσ in the stringer. Tack welds inside the shape of butt welds.
71		6) Critical section in web of cross girder due to cut outs.	6) Assessment based on stress range in critical section taking account of Vierendeel effects. **NOTE** In case the stress range is determined according to EN 1993-2, 9.4.2.2(3), detail category 112 may be used.
71	$\Delta\sigma = \frac{\Delta M_w}{W_w}$	Weld connecting deck plate to trapezoidal or V-section rib 7) Partial penetration weld with a ≥ t	7) Assessment based on direct stress range from bending in the plate.
50		8) Fillet weld or partial penetration welds out of the range of detail 7)	8) Assessment based on direct stress range from bending in the plate.

Finally, for an ergodic stress process, the scatter may be neglected and the damage can be expressed, for example, by

$$D = \frac{1}{A_1} \sum_{\Delta\sigma_i \geq \Delta\sigma_D} n_i \, \Delta\sigma_i^{m_1} + \frac{1}{A_2} \sum_{\Delta\sigma_D > \Delta\sigma_i > \Delta\sigma_L} n_i \, \Delta\sigma_i^{m_2} = \frac{1}{A_1} E\left[n(t)\right] E\left[\Delta\sigma^m\right] = \frac{1}{A_1} \psi_L(t) \tag{5}$$

where $\psi_L(t)$ may be referred to as the "fatigue loading".

In deterministic applications, Miner's rule stipulates that failure occurs when D is equal to unity but in the Probabilistic Model Code the critical value is also treated as a random variable.

2.2 Fracture Mechanics Approach

An alternative approach is based on the crack propagation laws determined using the fracture mechanics theory.

The general form of the crack propagation law under constant amplitude stress histories is

$$\frac{da}{dn} = f(\sigma, a, C) \tag{6}$$

where a is the crack length, n the number of cycles, da/dn is the crack propagation rate, σ is a representative value of the stress level and C a material constant. An example of a-N curves for increasing values of σ, $\sigma_{i+1} > \sigma_i$, is sketched in Figure 4: when $\sigma < \sigma_1$ the crack propagation rate is nil, while the critical crack length a_i corresponding to unstable propagation reduces as σ increases.

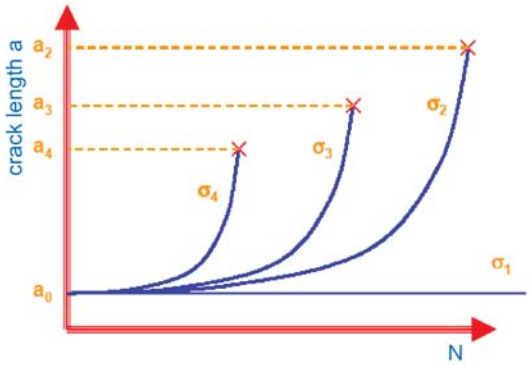

Figure 4 *a-N* curves for increasing values of σ

Generally, the crack propagation rate da/dn is expressed as function of the stress intensity factor range ΔK, which is the variation of the stress intensity factor in the stress cycle.

Recalling that the stress intensity factors are K_n for the three basic cases of stress at the crack tip are expressed by

$$K_j = Y_j \, \sigma_a \sqrt{\pi \, a} \tag{7}$$

where *j=I, II, III* is the basic case number (*I – opening*, *II – in-plane shear*, III – out-of-plane shear, see Figure 5), Y_j is the "geometry factor" and σ_a is the applied stress, derived from a detailed description of the stress system in the vicinity of the crack (but not influenced by it), ΔK_j for the basic cases can be expressed by

$$\Delta K_j = Y_j \, \Delta\sigma_a \sqrt{\pi \, a} \tag{8}$$

so that, it results

$$\Delta K = Y \, \Delta\sigma_a \sqrt{\pi \, a} \tag{9}$$

where ΔK depends on the applied loads, on the crack geometry and on the geometry of the element.

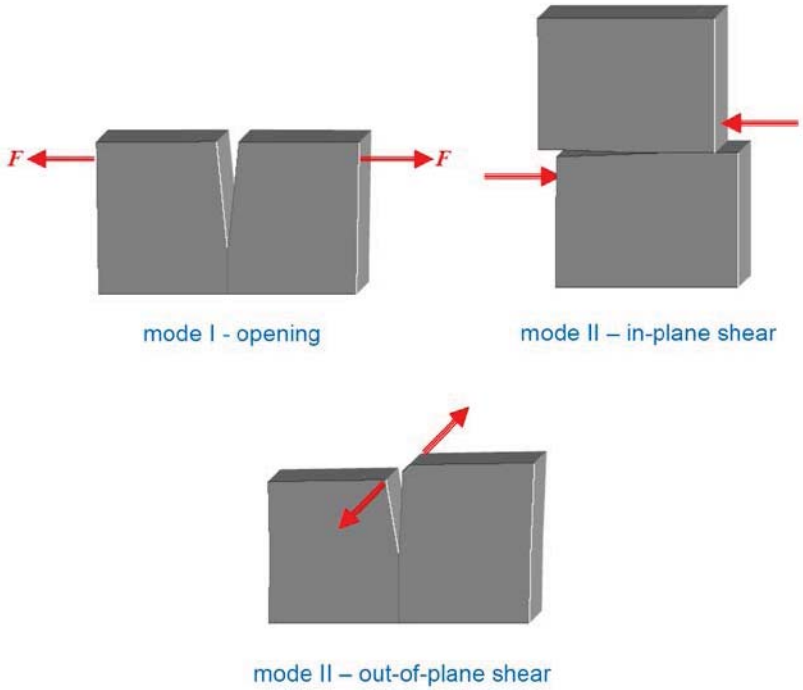

Figure 5 Basic modes of crack propagation

The most common model adopts the *Paris law* [13], which can be written as

$$\frac{da}{dn} = C\left(\Delta K^m\right) \tag{10}$$

being C and m material constants, which can be determined from experiments on simple specimens. The model can be improved by the introduction of a threshold value for ΔK, and, as in the *S-N* case, by considering different C and m parameters corresponding to particular ΔK ranges.

When ΔK can be assumed to be independent on t in a sinusoidal constant amplitude stress history and the critical length of the crack is much higher than the initial crack opening, the Expression (1) can be deduced from the Paris law (10).

Expression of ΔK can be determined by finite element analysis, directly or from the path-independent Rice integral, J [14].

For semi-elliptical cracks in plated structures, which are of interest in many practical applications, two crack dimensions, the depth a and the half-length at the surface c, both of which under fatigue are functions of the loading time t, need to be considered.

For both principal directions of the crack growth a Paris type expression is assumed, which, after integrating the differential equation from an initial defect size of a_0 to a crack size $a(t)$ after time t corresponding to an average number of stress cycles $E(n(t))$, leads to

$$\int_{a_0}^{a(t)} \frac{\sqrt{Q^m}\, dx}{C\, G(x) U_a^m\, Y_m^a \sqrt{\pi\, x^m}} = \sum \Delta\sigma^m = E\left[n(t)\right] E\left[\Delta\sigma^m\right] = \psi_L(t) \tag{11}$$

where $G(x)$ is the threshold correction factor, U_a is the effective stress intensity factor ratio, Q is the elliptic shape factor, and $\psi_L(t)$ (similar to the S-N approach) may be referred to as the "fatigue loading". When the fatigue life of a joint is required, the upper bound of the integral domain $a(t)$ in (11) may be taken as the critical value a_c or simply the plate thickness. Failure due to interaction between brittle fracture and section yielding is catered for through a failure assessment diagram.

3 EXAMPLE

Consider a bridge structure where various nodes are inspected for fatigue cracks. Failure in those cases will happen if the inspection results are considered as satisfactory but the failure event (nevertheless) occurs, assuming that some adequate action is taken if the inspection is not satisfactory. Let the fatigue crack for some selected node grow as indicated in Figure 6.

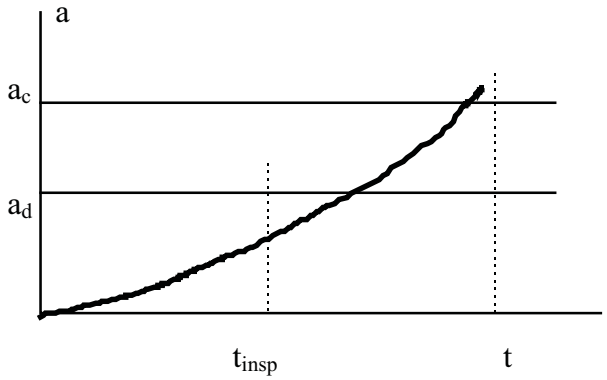

Figure 6 Fatigue failure before time t occurs if at inspection the crack length is smaller than a_d and at time t the crack length is larger than a_{crit}

Fatigue failure will occur as soon as the crack $a(t)$ reaches a random critical length a_{crit} so the failure probability for a period t can be written as:

$$P_F(t) = P\{M_f < 0\} = P\{a_{crit} - a(t) < 0\} \tag{12}$$

Note that a_{crit} is considered as time-independent; if a_{crit} is considered as time dependent (as it is in reality) this equation becomes more complex. Note also that $a(t)$ is an increasing stochastic process as cracks do not get smaller.

Let the reliability be considered as inadequate: that is, $P_F(t)>P_{tar}$, when P_{tar} is some target probability for fatigue failure. For this reason an inspection is planned at some point t_{insp} during the life time. Let the decision rule be that the structure will be repaired if a crack is detected, that is if a crack $a(t_{insp})$ larger than random detection limit a_d is detected.. The probability of failure, given a positive inspection can be written at time t_{insp}. as:

$$P_F(t) = P\{a(t) > a_{crit} \mid -a_m(t_{insp}) < a_m\} \tag{13}$$

If also cost values are attached to inspection and failure, the optimal time of inspection and repair level a_d can be found and decisions regarding the future use of the bridge can be taken as indicated in Figure 7.

Figure 7 Traffic constraints to avoid fatigue failure of metallic bridges

4 CONCLUSIONS

Fatigue assessment and evaluation of residual fatigue life of existing infrastructure have been summarized,

To design repair interventions of fatigue damaged details and planning of future maintenance and inspection programmes it must be pointed out that, since repair of fatigue cracked or damaged joint commonly restores only a part, and often a very low quota, of the original fatigue life, the definition of appropriate repair techniques should be one of the main outcomes of the fatigue assessment. In principle, successful fatigue crack repair techniques should combine satisfactory fatigue performance with simplicity, velocity and easiness of execution, aiming to achieve significant residual fatigue lives of repaired details minimising the total cost of the rehabilitation, which is the sum of the direct costs of repairs and of the indirect costs, due to the out of service or the service restrictions of the structure during the executions of the repairs themselves.

Clearly, cost reduction and repair effectiveness needs claim to lengthen profitably the time interval between two subsequent interventions, so that repairs should concern not only fatigue cracked joints, but also fatigue damaged ones, even if not yet cracked. Moreover, fatigue behaviour of repaired joints is often not known, so that it must be deduced by testing real scale specimens and compared with that of the corresponding virgin (undamaged) joints, also in the light of available literature, so that the fatigue behaviour of repaired details can be suitably identified.

REFERENCES

[1] ASTME 1150-87, Standard definitions of terms relating to fatigue. 1995 Annual Book of ASTM Standards. Vol. 03.01. ASTM. 753-762 (1995).

[2] ASM Handbook, *Fatigue and Fracture. Vol. 19*. Material, Parks: ASM (1996).

[3] Croce P. (2002) Background to fatigue load models for Eurocode 1: Part 2 Traffic loads, *Progress in Structural Engineering and Materials*, 3-2001, pp. 333-345.

[4] Manson S. S. (1953) Behavior of materials under conditions of thermal stress, NACA, TN-2933.

[5] Coffin L. F. (1954) A study of the effects of cyclic thermal stresses on a ductile metal. *Trans. ASME*, Vol. 76, 931-950.

[6] EN1993-1-9, Eurocode 3: Design of steel structures - Part 1-9: Fatigue, CEN, Brussels (2006).

[7] EN1993-2, Eurocode 3 - Design of steel structures - Part 2: Steel Bridges, CEN, Brussels, (2006).

[8] EN1999-1-3, Eurocode 9 - Design of aluminium structures - Part 1-3: Structures susceptible to fatigue, CEN, Brussels (2007).

[9] EN1992-1-1, Eurocode 2: Design of concrete structures - Part 1-1: General rules and rules for buildings, CEN, Brussels (2004).

[10] EN1992-2, Eurocode 2 - Design of concrete structures - Concrete bridges - Design and detailing rules, CEN, Brussels (2005).

[11] Palmgren, A (1924) Die Lebensdauer von Kugellagern, *Z. Vereins Deutscher Ingenieure*; Vol. 68: pp. 339-341.

[12] Miner M. A. (1945) Cumulative damage in fatigue. *Journal of Applied Mechanics*, Vol. 12: pp. A159-A164.

[13] Paris P. C., Erdogan F. (1963) A critical analysis of crack propagation laws. *Journal of Basic Engineering*, Vol. 85D, pp. 528-534.

[14] Rice J. R. (1968) A path independent integral and the approximate analysis of strain concentration by notches and cracks. *Journal of Applied Mechanics*, Vol. 35, pp. 379–386.